Biofuel cell based on glucose oxidase and microperoxidase-11 monolayer-functionalized electrodes

Itamar Willner,*,†,[a] Eugenii Katz,[a] Fernando Patolsky[a] and Andreas F. Bückmann[b]

[a] *Institute of Chemistry, The Hebrew University of Jerusalem, Jerusalem 91904, Israel*
[b] *Gesellschaft für Biotechnologische Forschung, Department of Molecular Structure, Mascheroder Weg 1, D-38124 Braunschweig, Germany*

Apoglucose oxidase was reconstituted onto a pyrroloquinoline quinone and flavin adenine dinucleotide phosphate, PQQ–FAD, monolayer associated with a rough Au electrode to yield a bioelectrocatalytically active glucose oxidase, GOx. Electrically contacted PQQ–FAD/GOx monolayer was applied to the biocatalytic oxidation of glucose. A microperoxidase-11, MP-11, monolayer was assembled onto a rough Au electrode and used for the biocatalytic reduction of H_2O_2. Both biocatalytic electrodes, Au/PQQ–FAD/GOx and Au/MP-11, were assembled into a biofuel cell using glucose and H_2O_2 as the fuel substrate and the oxidizer, respectively. The biofuel cell generates an open-circuit voltage, V_{oc}, of *ca.* 310 mV and a short-circuit current density, i_{sc}, of *ca.* 114 μA cm^{-2}. The maximum electrical power, P_{max}, extracted from the cell is 32 μW at an external optimal load of 3 kΩ. The fill factor of the biofuel cell, $f = P_{max} I_{sc}^{-1} V_{oc}^{-1}$, is *ca.* 25%.

Introduction

Biofuel cells use biocatalysts for the conversion of chemical energy to electrical energy.[1] As most organic substrates undergo combustion with the evolution of energy, the biocatalyzed oxidation of organic substances by oxygen at two-electrode interfaces provides a means for the conversion of chemical to electrical energy. Abundant organic raw materials such as methanol or glucose can be used as substrates for the oxidation processes at the anode, whereas molecular oxygen or H_2O_2 can act as the reduction substrate at the cathode. The extractable power (P) of a fuel cell is the product of the cell voltage (V_{cell}) and the cell current (I_{cell}). Although the ideal cell voltage is affected by the difference in the formal potentials of the oxidizer and fuel, irreversible losses in the voltage as a result of kinetic limitations of electron transfer at the electrode interfaces, ohmic resistances and concentration gradients, lead to decreased values of the cell voltage. Similarly, the cell current is controlled by the electrode sizes, the ion permeability and transport rate across the membrane separating the catholyte and anolyte compartments of the biofuel cell, and specifically, the rate of electron transfer at the respective electrode surfaces. These different parameters collectively influence the biofuel cell power, and for improved efficiencies the V_{cell} and I_{cell} values should be optimized.

Biofuel cells can use biocatalysts, enzymes or whole cell organisms in two different routes.[2] (i) The biocatalysts can generate the fuel substrates for the cell by biocatalytic transformations or metabolic processes. For example, the microorganism *Desulfovibrio desulfuricans* yields the metabolic reduction of sulfate to sulfide ions.[3] The latter product acts as the fuel substrate in the anodic compartment, where sulfide is being oxidized at the electrode interface to sulfate, and oxygen is reduced in the cathodic compartment of the fuel cell. Other microorganisms were reported to yield, by their metabolic activities, hydrogen, and the latter product was used as the substrate for the conventional H_2–O_2 fuel cell.[4] Alternatively, a series of enzymes, such as alcohol dehydrogenase, aldehyde dehydrogenase and formate dehydrogenase, transform methanol to carbon dioxide with the concomitant reduction of the 1,4-nicotinamide adenine dinucleotide, NAD^+, cofactor to its reduced form NADH.[5] The latter reduced cofactor acts as the fuel substrate for the anodic compartment of the fuel cell. (ii) The biocatalysts participate in the electron transfer chain between the fuel substrates and the electrode surfaces. That is, microorganisms or redox enzymes facilitate the electron transfer between the fuel substrate and the electrode interfaces, thereby enhancing the cell current. Most of the redox enzymes lack, however, direct electron transfer features with conductive supports, and a variety of electron mediators (electron relays) were used for electrical contacting of the biocatalysts and the electrode.[6] For example, *N*,*N*-dimethyl-7-amino-1,2-benzophenoxazinium cation, MB^+, was used as an electron mediator in the glucose oxidase biocatalyzed glucose–O_2 fuel cell.[7] Glucose acts as the anodic fuel and its biocatalyzed oxidation to gluconic acid yields the reduced glucose oxidase (GOx–$FADH_2$). The latter is oxidized by the electron mediator and the resulting electron carrier MBH_2 supplies the electrons for the cathodic reduction of oxygen.

In recent years, our laboratory has been extensively involved in the functionalization of electrode surfaces with monolayers consisting of redox enzymes,[8] electrocatalysts[9] and electrobiocatalysts[10] that stimulate electrocatalytic transformations at the electrode interfaces. Redox enzymes such as glucose oxidase or glutathione reductase were assembled as monolayers on Au electrodes and electrically contacted with the conducting supports by covalent tethering of electron relay units to the proteins.[8] Alternatively, reconstitution of apo-flavoenzymes, *e.g.* apoglucose oxidase, onto an electron mediator–FAD monolayer associated with an electrode, led to aligned biocatalysts on electrode surfaces exhibiting effective electrical contact.[11] Electron mediators, *e.g.* ferrocene units, were assembled as monolayers on electrode supports, and used to stimulate the electrical contact between redox enzymes and the electrode.[12] Similarly, redox-active biomaterials were assembled on electrode supports and used to activate biocatalytic electron transfer cascades, or to induce electrobiocatalyzed transformations.[10] For example, the heme-containing polypeptide microperoxidase-11, MP-11, was used to activate electron transfer to hemoproteins such as cytochrome c, Co^{II}-reconstituted myoglobin or nitrate reductase.[13]

The assembly of electrically contacted bioactive monolayer electrodes could be advantageous for biofuel cell applications as

† Fax: 972-2-6527715. Tel: 972-2-6585272. E-Mail: willnea@vms.huji.ac.il

the biocatalyst and electrode support are integrated. Recently we reported on the design of a biofuel cell based on the catalyzed oxidation of dihydronicotinamide adenine dinucleotide, NADH, by H_2O_2, using a microperoxidase-11 monolayer electrode and a pyrroloquinoline quinone, PQQ, monolayer-functionalized Au electrode as biocatalytic cathode and anode, respectively.[14] The electrical power that was extracted from the cell was 8 μW at an external load of 3 kΩ. The fill factor of this cell was *ca.* 25%.

Here we report on a novel biofuel cell configuration based on the biocatalyzed oxidation of glucose by H_2O_2 using a microperoxidase-11 monolayer electrode and an aligned glucose oxidase enzyme, reconstituted on a pyrroloquinoline quinone–flavin adenine dinucleotide phosphate, PQQ–FAD, monolayer on a Au electrode as biocatalytic cathode and anode, respectively. We found that the organized biofuel cell reveals a high electrical power that corresponds to 32 μW at an external load of 3 kΩ.

Experimental

Amino-functionalized FAD derivative, N^6-(2-aminoethyl)-FAD, was synthesized according to the recently published procedure.[15] Glucose oxidase, GOx, (E.C. 1.1.3.4, Sigma) was used to prepare the glucose oxidase apo-enzyme by the extraction of the native FAD-cofactor from the enzyme, followed by purification of the catalytically non-active apo-protein.[16] Pyrroloquinoline quinone (PQQ), microperoxidase-11 (MP-11), cystamine, 1-ethyl-3-[3-(dimethylamino)propyl]carbodiimide (EDC) and all other reagents were purchased from Aldrich. Ultrapure water from a Nanopure (Braunstead) source was used throughout this work.

Clean Au electrodes (wires 0.5 mm diameter, geometrical areas *ca.* 0.2 cm^2) were roughened (roughness factor *ca.* 15) and modified with a cystamine monolayer as reported previously.[17] The PQQ and MP-11 were covalently linked to amino groups of the cystamine monolayer in the presence of EDC as described previously.[17–19] The N^6-(2-aminoethyl)-FAD was covalently linked to the base cystamine monolayer in the presence of EDC and then the PQQ–FAD-functionalized electrode was used for reconstitution of glucose oxidase apo-enzyme.[11] The PQQ–FAD/reconstituted GOx and MP-11 monolayer modified electrodes were characterized using cyclic voltammetry using a potentiostat (EG&G VersaStat) connected to a personal computer (EG&G research electrochemistry software model 270/250). Cyclic voltammetry was performed under argon at ambient temperature in a three-compartment electrochemical cell consisting of the PQQ–FAD/reconstituted GOx or MP-11 modified electrode as the working electrode, a glassy carbon auxiliary electrode isolated by a glass frit and a saturated calomel electrode (SCE) connected to the working volume with a Luggin capillary. Cyclic voltammograms and potentiometric measurements for each modified electrode, in the presence of the corresponding substrate (glucose for PQQ–FAD/reconstituted GOx electrode and H_2O_2 for MP-11 modified electrode), are reported *vs.* SCE.

The same electrochemical cell, but in a two-electrode configuration, was used to measure the voltage and the current generated by the biofuel element consisting of PQQ–FAD/reconstituted GOx and MP-11 modified electrodes. The two compartments (cathodic and anodic) were separated by a glass frit. The substrates (glucose and H_2O_2) were added to the corresponding compartments of the cell. The voltage and the current generated by the cell were measured between the two modified electrodes by applying an external variable load resistance and using a Keithley Autoranging Microvolt DMM (Model 197) for the respective voltage and current measurements. The voltage and current outputs were measured under air.

Results and discussion

The assembly of the aligned glucose oxidase monolayer on a rough Au electrode (roughness factor *ca.* 15)[11] is shown in Scheme 1. A pyrroloquinoline quinone, PQQ, monolayer was assembled on a Au electrode by its coupling to a cystamine

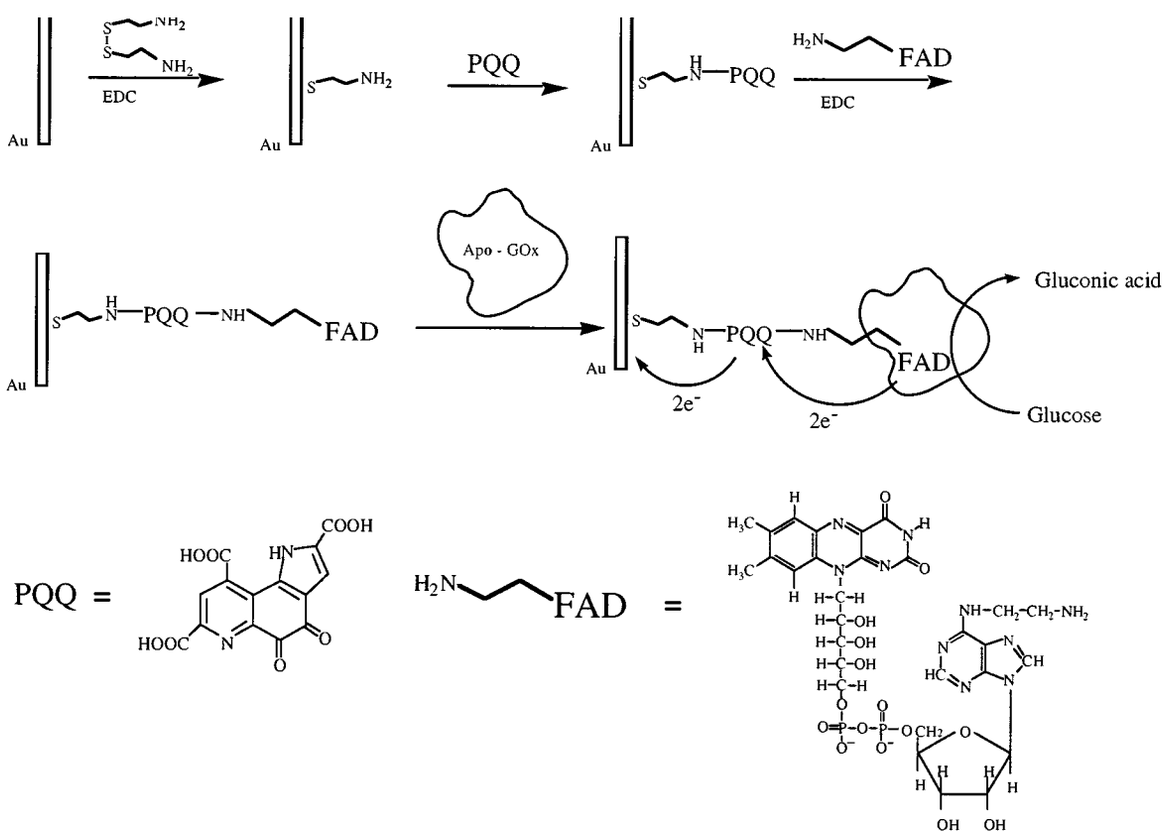

Scheme 1 Assembly of the reconstituted GOx on the PQQ–FAD monolayer-functionalized electrode

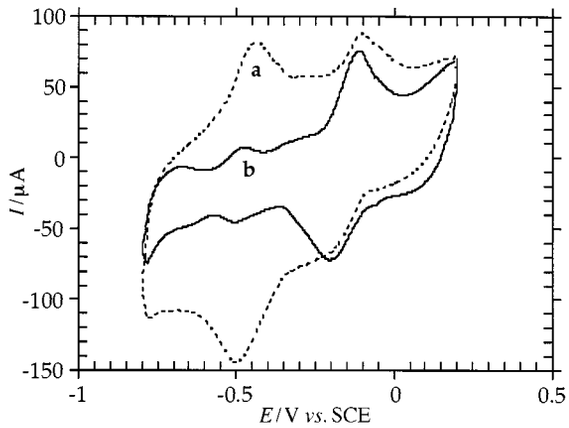

Fig. 1 Cyclic voltammograms of the PQQ–FAD monolayer on a Au electrode (a) before and (b) after reconstitution with apo-GOx. Ar atmosphere, 0.1 M phosphate buffer, pH 7.0. Potential scan rate, 50 mV s^{-1}.

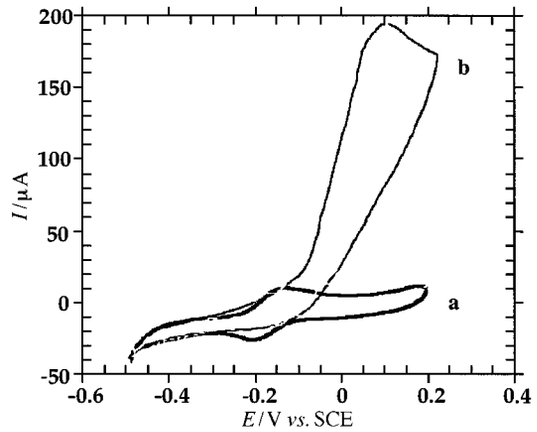

Fig. 2 Cyclic voltammograms of (a) glucose oxidase reconstituted on the PQQ–FAD monolayer bound to the gold electrode and (b) in the presence of added glucose, 5×10^{-3} M, and the PQQ–FAD-reconstituted GOx electrode. Ar atmosphere, 0.1 M phosphate buffer, pH 7.0. Potential scan rate, 5 mV s^{-1}.

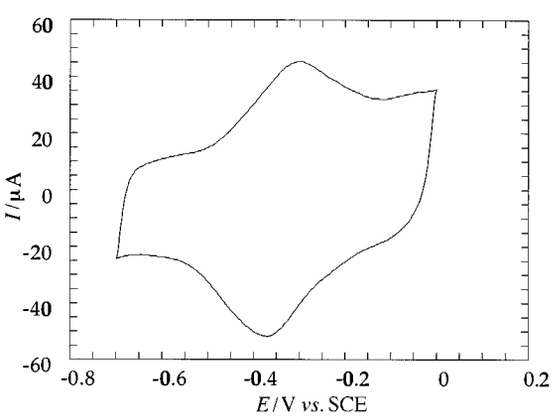

Fig. 3 Cyclic voltammogram of the MP-11 monolayer-modified Au electrode. Ar atmosphere, 0.1 M phosphate buffer, pH 7.0. Potential scan rate, 50 mV s^{-1}.

monolayer associated with a Au electrode. N^6-(2-Aminoethyl)-FAD was coupled to the PQQ monolayer, using 1-ethyl-3-[3-(dimethylamino)propyl]carbodiimide, EDC, as coupling reagent.[11] Cyclic voltammetry was applied to characterize the resulting PQQ–FAD monolayer assembly on the Au electrode. Two reversible redox waves corresponding to the two-electron redox processes of the PQQ and FAD units at formal potentials $E^\circ = -0.13$ V and $E^\circ = -0.50$ V (*vs.* SCE), at pH = 7.0, were observed (Fig. 1, curve a). Coulometric analysis of the reduction (or oxidation) waves of PQQ or FAD indicates that the surface coverage of the electrode by the PQQ and FAD units is 5.5×10^{-10} and 5.5×10^{-10} mol cm^{-2}, respectively. The interfacial electron transfer rate constants to the PQQ and FAD redox-active units were determined using Laviron's method,[20] by following the peak separation of the respective redox waves. The electron transfer rate constants to PQQ and FAD units are *ca.* 1 and *ca.* 5 s^{-1}, respectively. The resulting PQQ–FAD monolayer electrode was then treated with apoglucose oxidase, apo-GOx. This protein is obtained by the extraction of the native FAD cofactor from GOx. Surface reconstitution of apo-GOx on the PQQ–FAD monolayer occurs as a result of the association of apo-enzyme with the semisynthetic cofactor monolayer electrode. Reconstitution of the enzyme on the PQQ–FAD monolayer yields a bioelectrocatalytically active monolayer interface for the bioelectrocatalyzed oxidation of glucose. Fig. 1 (curve b) shows the cyclic voltammogram of the PQQ–FAD monolayer electrode after reconstitution with apo-GOx. The redox wave of the FAD unit is depleted, indicating its insulation by the associated enzyme. The redox wave of the PQQ unit is, however, visible after the association of apo-GOx with the monolayer, implying that the quinone unit is exposed to the electrode surface, and that electron transfer to it is retained. Fig. 2 shows the cyclic voltammogram of the reconstituted GOx monolayer electrode in the absence and presence of added glucose. With glucose, an electrocatalytic anodic current is observed, curve b, implying the effective bioelectrocatalyzed oxidation of glucose by the biocatalytic enzyme monolayer electrode. The anodic current transduced by the reconstituted GOx monolayer electrode is unprecedently high, and it is not affected by oxygen.[11] In a previous report[11] we estimated that the GOx biocatalyst reconstituted on the PQQ–FAD monolayer operates at a turnover rate of electron transfer close to the value of the native enzyme with dioxygen as electron acceptor. This extremely efficient electrical contact of reconstituted apo-GOx with the electrode is attributed to the alignment of the biocatalyst on the conductive support and the PQQ-mediated electron transfer between the FAD site and the electrode, Scheme 1. Oxidation of glucose by the biocatalyst yields the reduced $FADH_2$ redox site. The PQQ mediates oxidation of $FADH_2$ and further electron transfer to the electrode. As the quinone is exposed to the electrode surface, its rapid oxidation by the conductive support allows the cyclic electrochemically-induced oxidation of glucose.

Microperoxidase-11, MP-11, is an oligopeptide consisting of 11 amino acids and a covalently linked Fe^{III}-protoporphyrin IX heme site. The oligopeptide is obtained by the controlled hydrolytic digestion of cytochrome c and represents the structure of the active-site microenvironment of cytochrome c. We have previously reported on the assembly of an MP-11 monolayer on a Au electrode[18] and on the bioelectrocatalytic features of this monolayer in the reduction of H_2O_2,[19] organic peroxides,[9] and hemoproteins.[13] Scheme 2 shows the method of assembling the MP-11 monolayer electrode. It consists of the covalent coupling of the oligopeptide to a base cystamine monolayer in the presence of EDC. Fig. 3 shows the cyclic voltammogram of the resulting MP-11 monolayer. A quasi-reversible redox wave of the heme center of MP-11 is observed at $E^\circ = -0.40$ V (*vs.* SCE). Coulometric assaying of the redox wave indicates a surface coverage of 3×10^{-10} mol cm^{-2}. In a previous chronoamperometric characterization of the MP-11 monolayer electrode,[18] we identified two modes of binding the oligopeptide to the electrode support (*cf.* Scheme 2): (i) linkage of the carboxylic functions associated with the protoporphyrin IX ligand to the monolayer interface and (ii) coupling of carboxylic acid residues of the oligopeptide to the cystamine residues. These two modes of binding MP-11 to the monolayer reveal similar formal potentials. The electron transfer rates of the two binding modes of MP-11 were kinetically resolved, using chronoamperometry. The binding modes appear at an approximately 1 : 1

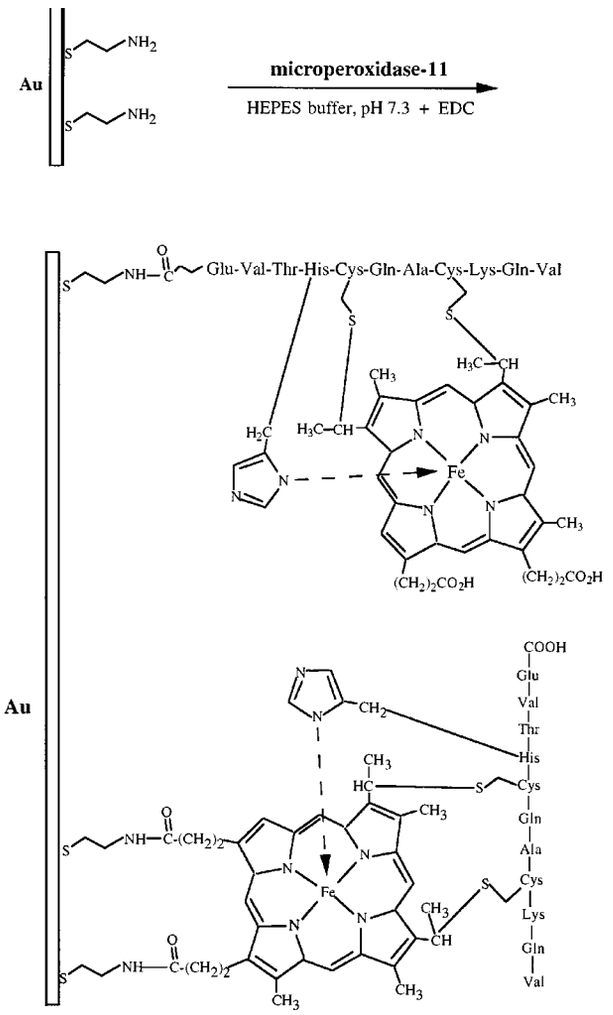

Scheme 2 Assembly of the MP-11 monolayer-modified electrode

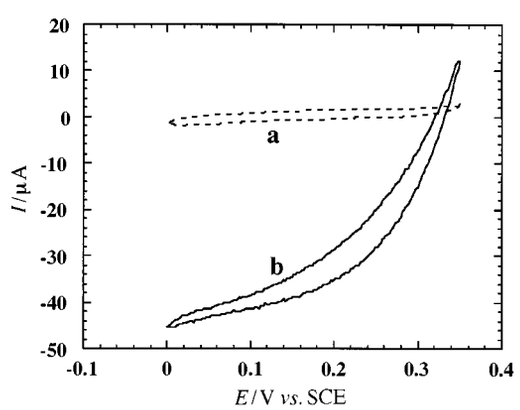

Fig. 4 Cyclic voltammograms of (a) the MP-11-functionalized electrode *vs.* background electrolyte and (b) the MP-11 modified electrode in the presence of H_2O_2, 5×10^{-3} M. Data recorded in 0.1 M phosphate buffer, pH 7.0. Potential scan rate, 5 mV s^{-1}.

ratio and the interfacial electron transfer rates to the two binding modes of the MP-11 are 8.5 and 16 s^{-1}. Fig. 4 shows the cyclic voltammograms of the MP-11-functionalized electrode in the absence of H_2O_2 (curve a) and in the presence of added H_2O_2 (curve b). The observed electrocatalytic cathodic current indicates the effective electrobiocatalyzed reduction of H_2O_2 by the functionalized electrode. Control experiments reveal that no electroreduction of H_2O_2 occurs at the bare Au electrode in this potential window.

The electrocatalyzed reduction of H_2O_2 by the MP-11 monolayer electrode and the effective electrobiocatalyzed oxidation

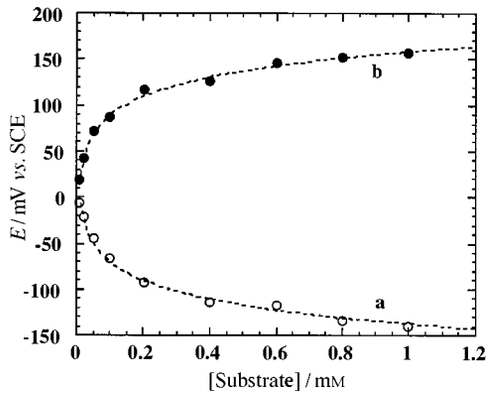

Fig. 5 (a) Potential of the PQQ–FAD/GOx-modified electrode as a function of glucose concentrations. (b) Potential of the MP-11-functionalized electrode as a function of H_2O_2 concentrations. Potentials were measured *vs.* SCE.

of glucose by the reconstituted GOx monolayer electrode permit, in principle, the design of biofuel cells using H_2O_2 and glucose as the cathodic and anodic substrates, respectively, Scheme 3. The MP-11 monolayer electrode acts as the cathode,

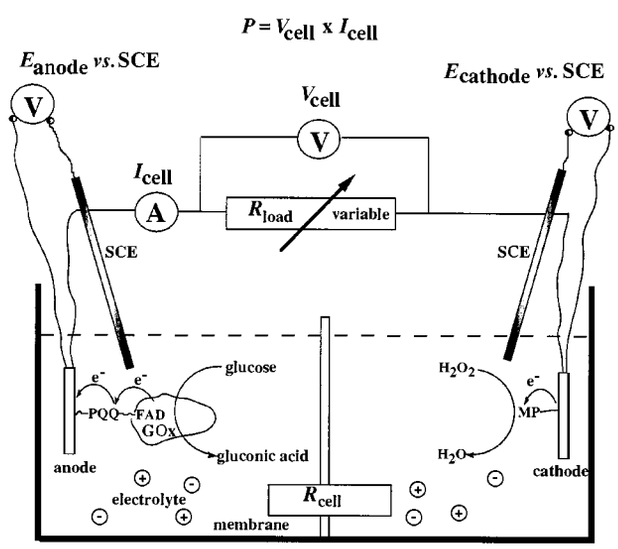

Scheme 3 Schematic configuration of a biofuel cell employing glucose and H_2O_2 as a fuel and an oxidizer, respectively, and PQQ–FAD/GOx and MP-11-functionalized electrodes as biocatalytic anode and cathode, respectively

whereas the GOx monolayer electrode is the anode of the biofuel cell element. For the optimization of the biofuel cell element, the potentials of the monolayer modified-electrodes as a function of the concentration of the cathodic and anodic substrates, were determined *versus* the SCE reference electrode. Fig. 5 shows the potentials of the GOx monolayer electrode at different concentrations of glucose (curve a) and the potentials of the MP-11 monolayer electrode at different concentrations of H_2O_2 (curve b). The potentials of the GOx monolayer electrode and of the MP-11 monolayer electrode become more negative and more positive as the concentrations of the glucose and H_2O_2 are elevated, respectively. The potentials of the electrodes reveal Nernstian-type behavior, reaching saturation at a high concentration of the substrates. For the specific system, the saturation potentials of the anode and cathode are reached at *ca.* 1×10^{-3} M of glucose and 1×10^{-3} M of H_2O_2, respectively. From the saturated potential values of the GOx and MP-11 monolayer electrodes, the theoretical limit of open-circuit voltage of the cell is estimated to be *ca.* 320 mV. The short-circuit current density generated by the cell was 340 μA. Taking into account the geometrical electrode area (0.2 cm^2)

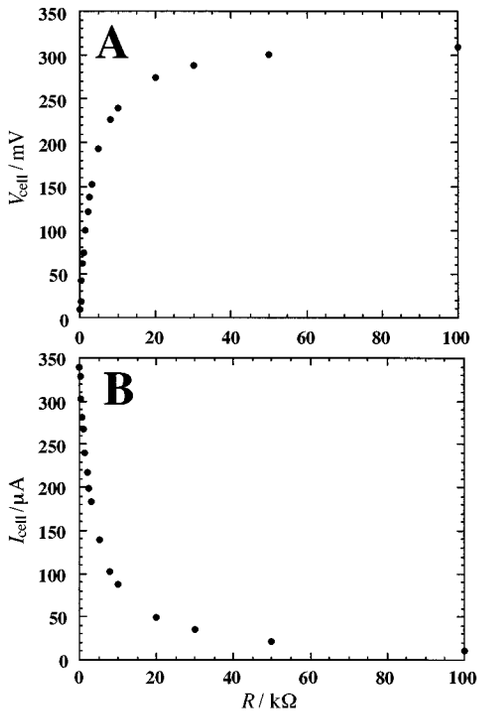

Fig. 6 (A) Biofuel cell voltage at different external loads. (B) Current developed by the cell at different external loads. Data recorded using the PQQ–FAD/GOx and MP-11 functionalized-electrodes and H_2O_2, 1×10^{-3} M, as the substrate solution in the cathodic compartment, and glucose, 1×10^{-3} M, as the substrate solution of the anodic compartment. The background electrolyte in both compartments was 0.1 M phosphate buffer, pH 7.0.

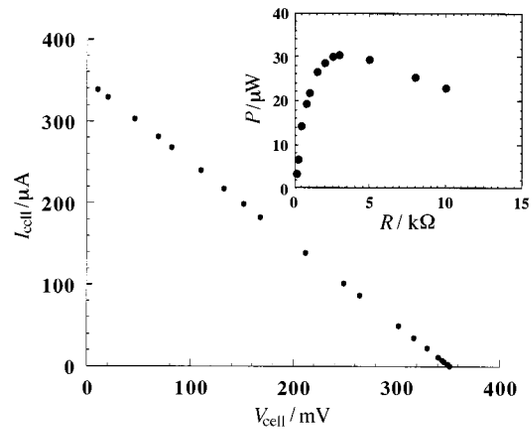

Fig. 7 Current–voltage behavior of the biofuel cell at different external loads. Inset: electrical power extracted from the biofuel cell at different external loads.

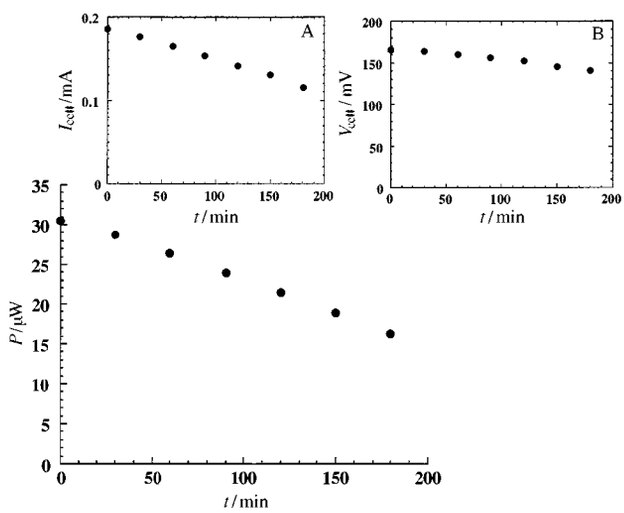

Fig. 8 Stability of the biofuel cell power operating at the optimal load of 3 kΩ as a function of time. Insets: (A) and (B) current and voltage, respectively, produced by the cell at the optimal load resistance 3 kΩ *vs.* time of operation. The measurements were performed using 10 mM solutions of glucose and H_2O_2 as initial concentrations of the fuel substrate and the oxidizer, respectively.

and the electrode roughness factor (*ca.* 15), the current generated by the cell can be translated into the current density, *ca.* 114 μA cm^{-2}. The theoretical limit of the current density extractable from the MP-11 monolayer electrode is *ca.* 300 μA cm^{-2} (MP-11 surface coverage × interfacial electron transfer rate × Faraday constant). For the GOx monolayer electrode the maximum extractable current density was estimated[11] to be *ca.* 100 ± 15 μA cm^{-2}. This value is based on the surface coverage of reconstituted GOx on the electrode, 1.7×10^{-12} mol cm^{-2}, and the theoretical turnover rate of electron transfer,[21] *ca.* 600 ± 100 s^{-1} of GOx with oxygen as electron acceptor. Thus, the observed short-circuit current density of the cell is probably controlled and limited by the bioelectrocatalyzed oxidation of glucose. This suggests that increasing the GOx content associated with the electrode could enhance the current density of the biofuel cell element and the extractable power.

The biofuel cell performance was examined at the concentration corresponding to 1×10^{-3} M of each of the two substrates: fuel and oxidizer. Fig. 6A shows the cell voltage at variable external loads. The cell voltage increases and at an external load of *ca.* 50 kΩ it levels off to a constant value of *ca.* 310 mV. Fig. 6B shows the resulting current in the cell at variable external loads. Upon increasing the external load, the current drops and is almost zero at an external load of 100 kΩ. Fig. 7 shows the current–voltage behavior of the biofuel cell at different external loads. The ideal voltage–current relationship for an electrochemical generator of electricity is rectangular.[22] The linear dependence observed for the biofuel cell has significant deviation from the ideal behavior and the fill factor of the biofuel cell, $f = P_{max}\, I_{sc}^{-1}\, V_{oc}^{-1}$, corresponds to *ca.* 25%. The theory of the various types of overvoltage which produce the non-rectangular *V–I* relationships has been addressed in detail by Vetter[23] and Delahay.[24] In the present case, the observed deviation results from mass transport losses[23,24] reducing the cell voltage below its reversible thermodynamic value. The power extracted from the biofuel element ($P = V_{cell}\ I_{cell}$) is shown in Fig. 7 (inset), for different external loads. The maximum power corresponds to 32 μW at an external load of 3 kΩ. It should be noted that the biofuel cell voltage and current outputs are identical under Ar and air. This originates from the effective electrical contact of the surface-reconstituted GOx with the electrode support, as a result of its alignment. This makes the enzyme insensitive to oxygen.[11]

The stability of the biofuel cell was examined as a function of time. Fig. 8 shows the power output of the cell, at an optimal loading resistance of 3 kΩ as a function of time. The power decreases by *ca.* 50% after *ca.* 3 h of the cell operation. This decrease in the cell power output could originate from the depletion of the fuel substrate, inter-penetration of the fuel and oxidizer into the respective counter compartments and the degradation of the biocatalysts included in the cell. Fig. 8, insets A and B, show the current output and voltage output of the cell as a function of time, respectively, using the optimal loading resistance (3 kΩ) that corresponds to the internal resistance of the cell (R_{cell}).[22] The current decreases by *ca.* 50% within 3 h of operation of the cell. At the same time interval, the cell voltage appears to be stable. Integration of the current output within these time intervals yields the charge that passes through the cell during the time of operation. We calculate that *ca.* 25% of the original fuel substrate concentration had been depleted upon operation of the cell for *ca.* 3 h. Thus, 25% of the total

decrease in the current output can be attributed to the consumption of the fuel substrate. This decrease in the current output could be compensated for by recharging the cell with the fuel substrate and oxidizer.

Conclusions

The present paper describes the use of monolayer-functionalized electrodes as catalytic interfaces for the organization of fuel cell elements. Specifically, we addressed the use of a glucose oxidase layer reconstituted onto a pyrroloquinoline quinone and flavin adenine dinucleotide, PQQ–FAD, monolayer, associated with a rough Au electrode as a bioelectrocatalytic interface for the oxidation of glucose. The system consists of the glucose oxidase monolayer electrode acting as anode and a microperoxidase-11 monolayer electrode acting as cathode. The glucose oxidase monolayer electrode drives the bioelectrocatalyzed oxidation of the glucose fuel substrate, whereas the microperoxidase-11 acts as the cathode for the biocatalyzed reduction of H_2O_2. The maximum power output of the cell is 32 μW at an optimal loading resistance of 3 kΩ.

Acknowledgements

This work was supported in part by the Volkswagen Stiftung, Germany.

References

1 (*a*) G. Prentice, *CHEMTECH*, 1984, **14**, 684; (*b*) G. Tayhas, R. Palmore and G. M. Whitesides, *ACS Symp. Ser. No. 566*, *Enzymatic Conversion of Biomass for Fuels Production*, 1994, ch. 14, pp. 271–290; (*c*) K. Kordesch, *Ber. Bunsen-Ges. Phys. Chem.*, 1990, **94**, 902; (*d*) C. Van Dijk, C. Laane and C. Veeger, *Recl. Trav. Chim. Pays-Bas*, 1985, **104**, 245; (*e*) S. Suzuki, I. Karube, H. Matsuoka, S. Ueyama, H. Kawakubo, S. Isoda and T. Murahashi, *Ann. N. Y. Acad. Sci.*, 1983, **413**, 133.

2 (*a*) W. J. Aston and A. P. F. Turner, *Biotechnol. Genet. Eng. Rev.*, 1984, **1**, 89; (*b*) E. V. Plotkin, I. J. Higgins and H. A. O. Hill, *Biotechnol. Lett.*, 1981, **3**, 187; (*c*) C. Laane, W. Pronk, M. Franssen and C. Veeger, *Enzyme Microb. Technol.*, 1984, **6**, 165; (*d*) C. A. Vega and I. Fernandez, *Bioelectrochem. Bioenerg.*, 1987, **17**, 217; (*e*) H. P. Bennetto, G. M. DeLaney, J. R. Mason, S. D. Roller, J. L. Stirling and C. F. Thurston, *Biotechnol. Lett.*, 1985, **7**, 699; (*f*) G. Kreysa, D. Sell and P. Kraemer, *Ber. Bunsen-Ges. Phys. Chem.*, 1990, **94**, 1042; (*g*) S. Tanisho, N. Kamiya and N. Wakao, *Bioelectrochem. Bioenerg.*, 1989, **21**, 25; (*h*) D. Sell, P. Kraemer and G. Kreysa, *Appl. Microbiol. Biotechnol.*, 1989, **31**, 211.

3 W. Habermann and E.-H. Pommer, *Appl. Microbiol. Biotechnol.*, 1991, **35**, 128.

4 I. Karube, T. Matsunaga, S. Tsuru and S. Suzuki, *Biotechnol. Bioeng.*, 1977, **19**, 1727.

5 (*a*) L. G. Lee and G. M. Whitesides, *J. Am. Chem. Soc.*, 1985, **107**, 6999; (*b*) I. Willner and D. Mandler, *Enzyme Microb. Technol.*, 1989, **11**, 467.

6 (*a*) G. Davis, H. A. O. Hill, W. J. Aston, I. J. Higgins and A. P. F. Turner, *Enzyme Microb. Technol.*, 1983, **5**, 383; (*b*) P. L. Yue and K. Lowther, *Chem. Eng. J.*, *Part B*, 1986, **33**, 69; (*c*) S. D. Roller, H. P. Bennetto, G. M. Delaney, J. R. Mason, S. L. Stirling and C. F. Thurston, *J. Chem. Technol. Biotechnol.*, *Part B*, 1984, **34**, 3.

7 B. Persson, L. Gorton, G. Johansson and A. Torstensson, *Enzyme Microb. Technol.*, 1985, **7**, 549.

8 (*a*) I. Willner, E. Katz, A. Riklin and R. Kasher, *J. Am. Chem. Soc.*, 1992, **114**, 10 965; (*b*) E. Katz, A. Riklin and I. Willner, *J. Electroanal. Chem.*, 1993, **354**, 129; (*c*) I. Willner, N. Lapidot, A. Riklin, R. Kasher, E. Zahavy and E. Katz, *J. Am. Chem. Soc.*, 1994, **116**, 1428; (*d*) I. Willner, A. Riklin, B. Shoham, D. Rivenzon and E. Katz, *Adv. Mater.*, 1993, **5**, 912; (*e*) B. Shoham, Y. Migron, A. Riklin, I. Willner and B. Tartakovsky, *Biosens. Bioelectron.*, 1995, **10**, 341.

9 A. N. J. Moore, E. Katz and I. Willner, *J. Electroanal. Chem.*, 1996, **417**, 189.

10 (*a*) I. Willner, E. Katz and B. Willner, *Electroanalysis*, 1997, **9**, 965; (*b*) E. Katz, V. Heleg-Shabtai, B. Willner, I. Willner and A. F. Bückmann, *Bioelectrochem. Bioenerg.*, 1997, **42**, 95.

11 I. Willner, V. Heleg-Shabtai, R. Blonder, E. Katz, G. Tao, A. F. Bückmann and A. Heller, *J. Am. Chem. Soc.*, 1996, **118**, 10 321.

12 (*a*) R. Blonder, E. Katz, Y. Cohen, N. Itzhak, A. Riklin and I. Willner, *Anal. Chem.*, 1996, **68**, 3151; (*b*) G. Tao, E. Katz and I. Willner, *Chem. Commun.*, 1997, 2073.

13 (*a*) A. Narvaez, E. Dominguez, I. Katakis, E. Katz, K. T. Ranjit and I. Willner, *J. Electroanal. Chem.*, 1997, **430**, 227; (*b*) V. Heleg-Shabtai, E. Katz and I. Willner, *J. Am. Chem. Soc.*, 1997, **119**, 8121; (*c*) V. Heleg-Shabtai, E. Katz, S. Levi and I. Willner, *J. Chem. Soc.*, *Perkin Trans. 2*, 1997, 2645.

14 I. Willner, G. Arad and E. Katz, *Bioelectrochem. Bioenerg.*, 1998, **44**, 209.

15 A. F. Bückmann, H. Erdmann, M. Pietzsch, J. M. Hall and J. V. Banniser, in *Flavins and Flavoproteins*, ed. K. Kuneoyagi, Walter de Gruyter, Berlin, 1994, pp. 597–609.

16 D. L. Morris and R. T. Buckler, in *Methods in Enzymology*, ed. J. J. Langone and H. Vunakis, Academic Press, New York, 1983, vol. 92, part E, pp. 413–417.

17 E. Katz, D. D. Schlereth and H.-L. Schmidt, *J. Electroanal. Chem.*, 1994, **367**, 59.

18 E. Katz and I. Willner, *Langmuir*, 1997, 13, 3364.

19 T. Lötzbeyer, W. Schuhmann, E. Katz, J. Falter and H.-L. Schmidt, *J. Electroanal. Chem.*, 1994, **377**, 291.

20 E. Laviron, *J. Electroanal. Chem.*, 1979, **101**, 19.

21 C. Bourdillon, C. Demaile, J. Gueris, J. Moiroux and J. Savéant, *J. Am. Chem. Soc.*, 1993, **115**, 12 264.

22 O'M. Bockris and S. Srinivasan, *Fuel Cells: Their Electrochemistry*, McGraw-Hill, New York, 1969, ch. 4.

23 K. J. Vetter, *Electrochemical Kinetics*, Academic Press, New York, 1967.

24 P. Delahay, *Double Layer and Electrode Kinetics*, Interscience, Wiley, New York, 1965.

Paper 8/01487F
Received 20*th February* 1998
Accepted 24*th April* 1998